YB-1 regulates tiRNA-induced Stress Granule formation but not translational repression

Published online 12 May 2016

Nucleic Acids Research, 2016, Vol. 44, No. 14 ***6949–6960***
doi: 10.1093/nar/gkw418

YB-1 regulates tiRNA-induced Stress Granule formation but not translational repression

Shawn M. Lyons[1,2], Chris Achorn[1], Nancy L. Kedersha[1,2], Paul J. Anderson[1,2,*] and Pavel Ivanov[1,2,3,*]

[1]Division of Rheumatology, Immunology and Allergy, Brigham and Women's Hospital, Boston, MA 02115, USA, [2]Department of Medicine, Harvard Medical School, Boston, MA 02115, USA and [3]The Broad Institute of Harvard and M.I.T., Cambridge, MA 02142, USA

Received January 06, 2016; Accepted April 30, 2016

ABSTRACT

Stress-induced angiogenin (ANG)-mediated tRNA cleavage promotes a cascade of cellular events that starts with production of tRNA-derived stress-induced RNAs (tiRNAs) and culminates with enhanced cell survival. This stress response program relies on a subset tiRNAs that inhibit translation initiation and induce the assembly of stress granules (SGs), cytoplasmic ribonucleoprotein complexes with cytoprotective and pro-survival properties. SG-promoting tiRNAs bear oligoguanine motifs at their 5′-ends, assemble G-quadruplex-like structures and interact with the translational silencer YB-1. We used CRISPR/Cas9-based genetic manipulations and biochemical approaches to examine the role of YB-1 in tiRNA-mediated translational repression and SG assembly. We found that YB-1 directly binds to tiRNAs via its cold shock domain. This interaction is required for packaging of tiRNA-repressed mRNAs into SGs but is dispensable for tiRNA-mediated translational repression. Our studies reveal the functional role of YB-1 in the ANG-mediated stress response program.

INTRODUCTION

Unfavorable environments trigger several stress response programs that promote the repair of stress-induced damage and enhance cell survival. Because protein synthesis is an energy-intensive process, inhibition of mRNA translation is a major component of these programs (1). Phosphorylation of eIF2α by any one of four stress responsive kinases (e.g. PERK, PKR, GCN4 or HRI) is the primary mechanism through which cells regulate global translation. Phosphorylation of Ser-51 of eIF2α inhibits GDP:GTP exchange by eIF2B, thereby blocking translation initiation (2). Translationally stalled ribonucleoprotein (RNP) complexes are organized into discrete cytoplasmic foci known as Stress Granules (SGs). In addition to conserving anabolic energy by preventing the synthesis of housekeeping proteins, SGs promote cell survival by sequestering pro-apoptotic signalling proteins (e.g. RACK1 and TRAF2) and promoting the translation of a select group of mRNAs harboring upstream open reading frames (uORFs) or internal ribosome entry sites (IRESes) (3). Translation of stress-activated IRES-containing mRNAs, such as BCL-2, or uORF-containing mRNAs such as ATF4, contributes to the survival of cells exposed to adverse environmental conditions (4).

Phospho-eIF2α independent triggers of SG assembly include eIF4A inhibitors (5) and hypertonic stress (6). We have discovered that stress-induced tRNA cleavage also triggers phospho-eIF2α independent SG assembly (7–9). In response to specific environmental stresses, a small percentage of tRNA (∼1%) is cleaved within anti-codon loops by angiogenin (ANG), a stress-activated ribonuclease (RNase) (8,10,11). tRNA cleavage produces two small non-coding (nc)RNAs that we have termed 5′- and 3′-tRNA derived stress-induced RNAs (5′- or 3′-tiRNAs) (8). In our initial analysis of tiRNA bioactivity, we discovered that a subset of 5′-tiRNAs, but not 3′-tiRNAs, inhibits global translation. Inhibition of mRNA translation is not sequence-dependent as it does not rely on RNA:RNA base pairing as with miRNA-mediated inhibition. These bioactive 5′-tiRNAs inhibit translation initiation by displacing eIF4F from the m^7GTP cap of mRNAs, thereby inhibiting cap-dependent translation and triggering the phospho-eIF2α independent assembly of SGs (9). The ability of bioactive 5′-tiRNAs to displace eIF4F from mRNAs is dependent upon a 5′-terminal oligoguanine (5′-TOG) motif that folds into G-quadruplex-like structures (9,12). Two 5′-tiRNAs, 5′-tiRNA^{Ala} and 5′-tiRNA^{Cys}, contain this motif and are able to inhibit translation and trigger the formation of SGs. ANG treatment, which induces the production of endoge-

*To whom correspondence should be addressed. Tel: +1 617 525 1233; Fax: +1 617 525 1310; Email: pivanov@rics.bwh.harvard.edu
Correspondence may also be addressed to Paul J. Anderson. Tel: +1 617 525 1202; Fax: +1 617 525 1310; Email: panderson@rics.bwh.harvard.edu

nous tiRNAs, or transfection with exogenous DNA analogues of 5′-TOG-containing tiRNAs, promotes the survival of motor neurons in response to excitotoxic or serum withdrawal associated stresses (12).

RNA affinity chromatography followed by mass spectroscopy identified the multifunctional cold-shock domain (CSD)-containing Y-box binding protein 1 (YB-1, YBX1) as a component of the 5′-TOG-tiRNA RNP (9). CSD-containing proteins bind both DNA and RNA and are involved in diverse RNA metabolism pathways. Examples include Lin28 which regulates pre-let7 miRNA biogenesis, and Upstream of N-Ras (UNR/CSDE1) which regulates mRNA translation and stability (13). The YB-1 CSD binds 5′-tiRNA in a sequence specific manner. YB-1 also possesses an oligomerization domain (OMD) that binds RNA in a sequence non-specific manner. Whereas a single YB-1 polypeptide is ∼35 kDa, the OMD promotes the assembly of 800–1000 kDa aggregates (14). Similar to other CSD proteins, YB-1 is an established regulator of translation. At low concentrations, YB-1 is thought to promote the translation of mRNAs to which it is bound, but at higher concentrations, it inhibits translation (15). This activity is likely due to the ability of YB-1 to dissociate eIF4G from mRNAs (16).

YB-1 has been implicated in many pathological states; notably, it is highly expressed in many cancers and its expression is positively correlated with increased metastasis and survival (17–19). This is likely due to its ability to promote an epithelial-to-mesenchymal transition (EMT), a dedifferentiated state that promotes cell migration and metastasis (20,21). YB-1 overexpression in epithelial MCF10AT cells bestows mesenchymal-like properties including increased invasion through soft agar, disruption of round, ordered acini structures in 3D culture and alteration of gene expression. These changes are accompanied by increased expression of EMT-associated transcription factors such as Twist1 and Snail1 (18,21). In its cytoplasmic role, YB-1 is a component of SGs and it has been reported to promote SG assembly in a G3BP1-dependent manner (22).

Precisely how 5′-TOG-containing tiRNAs displace eIF4F and promote SG assembly is unknown. Here, we investigate the role that YB-1 plays in tiRNA-mediated translational control. Using YB-1 knockout cells generated by CRISPR/Cas9, we show that YB-1 is required for SG formation in response to 5′-TOG-containing tiRNAs. This activity is dependent upon YB-1 binding to 5′-TOG-containing tiRNAs though it's CSD. In contrast, YB-1 is dispensable for tiRNA-mediated eIF4F displacement and translation inhibition. This work identifies the step at which YB-1 functions in the tiRNA pathway. We also describe a YB-1 frameshift mutation found in several cancer cell lines whose independent selection suggests a possible role in the cancer phenotype.

MATERIALS AND METHODS

Antibodies

The following antibodies were used for Western blotting and immunofluorescence: YB-1 (Abcam: Ab12148, Proteintech Group: 20339-1-AP, Bethyl Laboratories, Inc (A): A404-230-T, Bethyl Laboratories, Inc (B): A303-231-T), Dach1 (Proteintech Group: 10914-1-AP), Caprin1 (Proteintech Group: 14112-1-AP), G3BP1 (Santa Cruz Biotechnology, Inc: sc-81940), G3BP2 (Bethyl Laboratories, Inc: A302-040A), TIA-1 (Santa Cruz Biotechnology, Inc: sc-1751), TIAR (Santa Cruz Biotechnology, Inc: sc-1749), eIF3b (Santa Cruz Biotechnology, Inc: sc-16377), eIF4G (Santa Cruz Biotechnology, Inc: sc-11373), eIF4E-BP1 (Cell Signaling Technology: 9452S), PABP (Santa Cruz Biotechnology, Inc: sc-32318), Nucleolin (Santa Cruz Biotechnology, Inc: sc-9893), eIF4E (Santa Cruz Biotechnology, Inc: sc-9976), HuR (Santa Cruz Biotechnology, Inc: sc-5261), Fxr2 (Santa Cruz Biotechnology, Inc: sc32266), Rack1 (Santa Cruz Biotechnology, Inc: sc-17754), RPS23 (Santa Cruz Biotechnology, Inc: sc-100837), Twist1 (Bethyl Laboratories, Inc: A301-394A), Snail1 (Origene: TA500416), Zeb1 (Bethyl Laboratories, Inc: A301-921A), Puromycin (EMD Milipore: 12D10), GFP (Applied Biological Materials: G160), β-actin (Proteintech Group: 66009-1).

CRISPR/Cas9 mediated knockout of YB-1

Oligonucleotides encoding gRNAs targeting the first exon of YB-1 were designed using CRISPR Design software from the Zhang lab (crispr.mit.edu). Oligonucleotides were annealed and cloned into pCas-Guide (Origene) according to manufacturer's protocol. gRNAs target the following sequences within YB-1: gRNA1, AGCGCCGCCGAC ACCAAGCC; gRNA2, CGACACCAAGCCCGGCAC TA; gRNA3, GACACCAAGCCCGGCACTAC; gRNA4, AAGCCCGGCACTACGGGCAG. pCas-guide plasmids with cloned with gRNAs were transfected into U2OS or MCF7 cells using Lipofectamine 2000 (Invitrogen). Cells were allowed to recover for seven days and then immunostained for YB-1 to determine the percentage of knockouts. MCF7 cells were first 'pool cloned' to enrich knockouts by plating 5–10 cells per well in a 24-well plate. Pool clones were screened by immunofluorescence. Pool cloned MCF7 cells and original transfection of U2OS were cloned by limiting dilution and screened by immunofluorescence and Western blotting.

siRNA knockdown

U2OS cells (100 000 cells/well) were seeded in 6-well plates and grown for 24 h. The first round of siRNA transfection was using 100 pmol siRNA (SmartPool, Dharmacon), 2.5 μl Lipofectamine 2000 (Invitrogen) in OPTI-MEM (Life Technologies). The second transfection was done 48 h later with the same conditions as the first one.

Genotyping of YB-1

Cells were resuspended at 10^8 cells/ml in digestion buffer (100 mM NaCl, 10 mM TRIS [pH 8.0], 25 mM EDTA [pH 8.0], 0.5% SDS, 0.1 mg/ml proteinase K) and incubated overnight at 55°C. DNA was extracted with phenol/chloroform and precipitated with ammonium acetate and 2 volumes of 100% ethanol, washed with 70% ethanol and air dried. DNA pellet was resuspended in TE buffer containing 0.1% SDS and RNase A (1 μg/ml) and incubated at 37°C for 1 h. DNA was extracted with

phenol/chloroform and precipitated as described above. Resulting pellet was resuspended at a concentration of 100 ng/μl.

For genotyping, the first exon of YB-1 was amplified by polymerase chain reaction (PCR) using primers located within the promoter and first intron (Forward: GGTCCAATGAGAATGGAGGA, Reverse: AGCTCCGGCTAACGGTTC) using Accuprime G–C rich polymerase (Invitrogen). Amplicons were sequenced directly or cloned into pGEM–T Easy vector (Promega) and sequenced individually.

Stress granule induction and quantification

Stress granules were induced using sodium arsenite or thapsigargin at indicated concentrations for 1 h. Alternatively, cells were transfected with 250 pmol of indicated RNA for 6 h using Lipofectamine 2000 (Invitrogen). Cells were manually scored for SGs using fluorescence microscopy with eIF4G, TIAR and G3BP1 as SG markers (23). Only cells with granules co-staining for all three markers were considered SGs, and a minimum of 3 SGs per cell were required to score positive.

Immunofluorescence

Cells were fixed and processed for fluorescence microscopy as described previously (23). Briefly, cells were grown on glass coverslips, stressed as indicated and fixed with 4% paraformaldehyde in PBS (phosphate buffered saline) for 15 min followed by 10 min post-fixation/permeabilization in −20°C methanol. Cells were blocked for 1 h in 5% horse serum/PBS. Primary and secondary antibody incubations were performed in blocking buffer for 1 h with rocking at room temperature. Secondary antibodies (Jackson Laboratories) were tagged with Cy2, Cy3 or Cy5. Following washes with PBS, cells were mounted in polyvinyl mounting media and viewed at room temperature using a Nikon Eclipse E800 microscope with a 40X Plan fluor (NA 0.75) or 100X Plan Apo objective lens (NA 1.4) and illuminated with a mercury lamp and standard filters for DAPI (UV-2A - 360/40; 420/LP), Cy2 (FITC HQ 480/40; 535/50), Cy3 (Cy 3HQ 545/30; 610/75) and Cy5 (Cy 5 HQ 620/60; 700/75). Images were captured with SPOT Persuit digital camera (Diagnostic Instruments) with the manufacturers software and compiled using Adobe Photoshop CC 2015.

m^7GTP binding assay

eIF4F was assembled onto m^7GTP-agarose (Jena Bioscience) as previously described (9). Assembled eIF4F complexes were challenged with 100 pmol of indicated RNA for 2 h at 4°C while tumbling. Displaced proteins were washed away with NP-40 lysis buffer (10 mM Tris [pH 8.0], 100 mM NaCl, 0.5% NP-40, 1 mM EDTA) and bound proteins were eluted with 60 μl of 1X SDS-Loading dye. eIF4F displacement was assessed by analyzing eIF4G and eIF4E by western blotting.

Cloning and purification of recombinant YB-1

Human YB-1 was amplified from human cDNA prepared using Superscript III (Invitrogen) according to manufacturer's instructions and cloned into pET42 between BamHI and XhoI using the following DNA oligonucleotides: ttttggatccATGAGCAGCGAGGCCGAG (forward) and ttttctcgagTTACTCAGCCCCGCCCTG (reverse). The YB-1 (1-129) fragment was subcloned into pET42 between BamHI and XhoI using the following oligonucleotides: ttttggatccATGAGCAGCGAGGCCGAG (forward) and ttttctcgagttaACCAGGACCTGTAACATTTG (reverse). For F85A mutation, overlap PCR was used (24). Resulting mutated amplicons were cloned into pET42 between BamHI and XhoI. All vectors were confirmed by DNA sequencing.

For protein expression, BL21(DE3) *E. coli* were transformed with either pET42-YB1 (1-129) or pET42-YB1 (1-129)-F85A. Individual clones were picked and grown overnight. The following day 500 ml cultures were inoculated with 25 ml of overnight culture and grown until OD^{600} = 0.4–0.6. Cultures were induced with 0.5 mM IPTG for 4 h and harvested by centrifugation. His-tagged YB-1 was purified using Ni-NTA agarose (Qiagen) using non-denaturing conditions according to manufacturer's instructions.

Electrophoretic mobility shift assay (EMSA)

Electrophoretic mobility shift assays (EMSA) were performed as previously described (25). RNA was end-labeled with γ-^{32}P-ATP (Perkin Elmer) using T4 PNK followed by purification through G-25 Sephadex. For each shift, 0.25 pmol of RNA was used. The RNA was incubated on ice with various amounts of purified recombinant protein in 10 mM HEPES [pH 7.6], 50 mM KCl, 0.1 mM EDTA, 10% glycerol, 0.5 μg yeast tRNA, 0.1 μg/μl BSA. Reactions were loaded directly onto native polyacrylamide gel (acrylamide:bisacrylamide 29:1 in 1X TBE/5% glycerol). The radioactive complexes were visualized by autoradiography.

In vitro translation assay

U2OS cells were grown in 100 mm dishes until ∼75% confluent. Cells were removed from dish by trypsinization, washed in DMEM containing 10% fetal bovine serum (FBS) to neutralize trypsin. Cells were washed two times in HBSS to remove DMEM. Cells were diluted to 8×10^7 cells/ml in Lysolecitin buffer (20 mM HEPES-KOH [pH 7.4], 100 mM KOAc, 2.2 mM $Mg(OAc)_2$, 2 mM DTT, 0.1 mg/ml lysolecitin) and incubated on ice for 1 min. Cells were pelleted by centrifugation for 10 s at 10000 x*g*. Supernatant was discarded and cells were resuspended in 0.5 ml of hypotonic extraction buffer (20 mM HEPES-KOH [pH 7.4], 10 mM KOAc, 1 mM $Mg(OAc)_2$, 4 mM DTT, 1X protease inhibitor (Thermo Scientific) and incubated on ice for 5 min. Cells were disrupted by passage through a 27-gauge needle 10 times. Cell debris was pelleted for 10 min by centrifugation at 10000 x*g*. Supernatant was removed to new tube, aliquoted, quick frozen on dry ice and stored at −80°C until needed.

The plasmid phRL-5BoxB (encoding luciferase mRNA reporter) was linearized with XhoI; *Renilla* luciferase RNA was transcribed using T7 RiboMax Express Large Scale RNA Production System (Promega). RNA was phenol/chloroform extracted, precipitated with ammonium acetate, resuspended in ddH_2O and further purified

by removing unincorporated nucleotides by G-25 Sephadex size exclusion chromatography. Resulting RNA was diluted to 100 ng/μl.

Translation reactions were carried out as previously described (26). For *in vitro* translation reactions, 1 μl of *Renilla* luciferase mRNA reporter (100 ng/μl), 4 μl of translation extract, 0.2 μl of RNasin (Promega), 2 μl of 5X Translation buffer (100 mM HEPES-KOH [pH 7.6], 5 mM DTT, 2.5 mM Spermidine-HCl, 3 mM $Mg(CH_3COO)_2$, 40 mM creatine phosphate, 5 mM ATP, 1 mM GTP, 600 mM KCH_3COO, 125 μM amino acids) and 1 μl of indicated control RNA (three unrelated control RNAs we used: Ctrl1, Ctrl2 and D0R0; all 100 μM) or 5′-tiRNA^{Ala} (100 μM) were mixed and brought to 10 μl with ddH_2O. Reactions were incubated at 30°C for 1 h. Luciferase activity was assayed using *Renilla* Luciferase assay kit (Promega) on Moonlight Luminometer (BD Biosciences) according to manufacturer's instructions (2 s measurement delay followed by 10 s measurement time).

Ribopuromycilation assay

Cells were treated with indicated stresses for indicated times. Five minutes prior to harvesting, puromycin was added to cell media to a final concentration of 5 μg/ml. Puromycin was allowed to incorporate into *de novo* synthesized proteome for 5 min. Cells were washed 1X with HBSS and complete cell lysis was performed using 1% SDS, 5 mM MES [pH 6.5]. Western blotting was performed on lysates using anti-puromycin antibody to detect *de novo* protein synthesis after cellular stress and anti-actin for normalization. Blots were quantified, normalized to actin loading and plotted relative to untreated control.

RESULTS

Generation of ΔYB-1 cell lines

To analyze the extent to which YB-1 is required for cellular functions of 5′-TOG-containing tiRNAs, we created genetic nulls of YB-1 in human osteosarcoma (U2OS) and breast cancer (MCF-7) cell lines using CRISPR/Cas9 technology (27,28). CRISPR design software (crisper.mit.edu) was used to design gRNAs targeting the 1st exon of YB-1 within the coding sequence (Figure 1A). We obtained clonal YB-1 knockout cell lines (ΔYB-1) through limiting dilution subcloning and screening by immunofluorescence. Knockouts were confirmed by western blotting using four different polyclonal YB-1 antibodies (Figure 1B) raised to different regions of the protein (Supplementary Figure S1A). In these ΔYB-1 cells, we asked whether SG components, translation initiation factors, general RNA binding proteins or DACH1, the inhibitor of YB-1 (29), were altered by YB-1 deletion (Figure 1B). We found no YB-1 dependent difference in the levels of any interrogated protein. This is in contrast to recently published data by the Sorenson lab, which reported that siRNA mediated knockdown of YB-1 leads to decreased levels of G3BP1, a key SG regulator (30), thus inhibiting SG formation in response to arsenite or H_2O_2 (22). To address whether this disparity is due to differences between transient siRNA knockdown (their study) and genetic CRISPR/Cas9 mediated knockout, we performed siRNA knockdown of YB-1 to determine whether G3BP1 levels were affected. Despite efficient knockdown of YB-1, we failed to see any discernable difference in the levels of G3BP1 or DACH1 (Figure 1C and D). Moreover, CRISPR/Cas9-mediated targeting of YB-1 by three independent guide RNAs did not affect G3BP1 levels or sodium arsenite (SA)-induced SG formation in YB-1-depleted cells (Supplementary Figure S2). We also confirmed that YB-1 was disrupted at the DNA level by sequencing PCR amplicons using primers within the promoter and intron 1 (Figure 1A) in ΔYB-1 cells. We determined that a single adenosine insertion (256insA) caused a frameshift mutation, thereby ablating full length YB-1 expression (Figure 1E).

Genetic Heterogeneity of YB-1

While analyzing the ΔYB-1 cells, we also sequenced wild-type U2OS and, surprisingly, we found heterogeneity at the WT YB-1 locus. One allele in WT U2OS harbored the same 256insA frameshift mutation as did the ΔYB-1 cells. Sequencing in both directions confirmed that this frameshift occurred due to a single adenosine insertion at RNA nucleotide position 256 (256insA) (Figure 2A). Furthermore, PCR products were cloned and sequenced demonstrating the existence of two different alleles of YB-1, including one with a single nucleotide insertion (Supplementary Figure S1B and C). This insertion creates an RNA that encodes a hypothetical 8 kDa protein including the first 28 amino acids of YB-1 and unique sequence downstream (Figure 2B). We extended our analysis to other common cancer cell lines and were surprised to find that MCF-7, Jurkat and DU145 cells are heterozygous for the 256insA mutation, whereas HeLa-S cells are homozygous WT (Figure 2C, Supplementary Figure S1D–G). We hypothesized that mRNA encoding this protein would be inefficiently translated, as the frameshift causes a premature termination codon (PTC) upstream of six exon junctions, thereby making it a target for nonsense-mediated mRNA decay (NMD). To determine if this is true, we generated a series of reporter plasmids (Figure 2D) encoding YFP-tagged YB-1 cDNA [pEYFP-YB1(WT)], YFP-tagged YB-1 containing full length introns 4 and 5 [pEYFP-YB1 (In4+5)] and this same construct harboring the 256insA frameshift [pEYFP-YB1(In4+5/256insA)]. We transfected these plasmids into U2OS cells along with an empty pEYFP plasmid and analyzed the expression of each construct by Western blotting. We confirmed that insertion of two introns does not alter the expression of tagged YB-1 (Figure 2E, c.f. lane 3 and 4) by western blotting for both YB-1 and YFP. YFP-YB1 (In4+5/256insA) does not accumulate as either tagged YB-1 constructs or free YFP (Figure 2E, lane 2). Only overexposed blots are we able to detect any protein produced by this construct (Figure 2E, lane 5). It is likely that the reduced expression is due to NMD of the mRNA; however, it is also possible that the 256insA protein is inherently unstable. Because gRNAs used to generate YB-1 knockout cells overlapped with 256insA (Supplementary Figure S1B), the mutated allele would not be targeted by gRNA:Cas9 complexes (31). Following Cas9-mediated double strand break, repair was completed by homologous recombination using

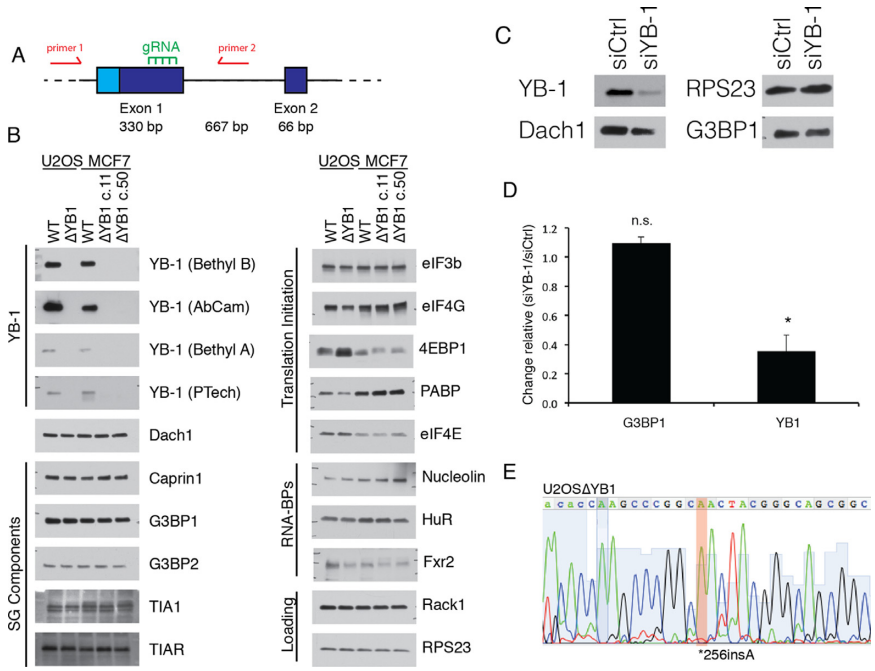

Figure 1. Creation of ΔYB1 cells. (**A**) CRISPR/Cas9 mediated deletion of YB-1 utilizing guide RNA located within the YB-1's 1st exon. Green line indicates location of gRNA and red arrows denote primers used for sequencing. (**B**) Western blotting confirming the loss of YB-1 expression, while other stress granule proteins, translation factors and general RNA binding proteins are unaffected. Ribosomal proteins Rack1 and RPS23 serve as loading controls. (**C**) siRNA-mediated knockdown of YB-1 confirms that G3BP1 levels are unaffected by depletion of YB-1. In addition, levels of Dach1 are unaltered. RPS23 serves as a loading control. (**D**) Quantification of relative change in levels of YB-1 and G3BP1 (siYB1/siCtrl) in response to RNAi mediated depletion of YB-1 confirms no change in G3BP1 levels. Levels of each protein are normalized to RPS23 (* *P*-value =0.0039, n=3). (**E**) CRISPR/Cas9 mediated deletion of YB-1 occurs by insertion of a single adenosine nucleotide at position 256 of the YB-1 gene. Homozygous insertion is highlighted in red.

256insA as a template, thereby converting cells to homozygous 256insA (Figure 1E) and null for YB-1 protein as determined by western blotting (Figure 1B).

YB-1 knockouts show decreased proliferative and cell survival responses

YB-1 has multiple reported growth phenotypes (18,32); therefore, we began our analysis of ΔYB-1 cells by determining their growth rates relative to WT cells. We found a significant difference in the growth rates of ΔYB-1 versus WT cells. ΔYB-1 U2OS cells consistently exhibit ∼25% slower growth than WT cells (Figure 3A), and this growth defect is enhanced under low serum (0.1%) conditions (Figure 3B and D). In addition, low serum causes ΔYB-1 cells to undergo dramatic morphological changes (Figure 3B, c.f. 2Bb and 2Bd), an effect that was not observed in serum-starved WT cells (Figure 3B, c.f. 2Ba and 2Bc).

YB-1 promotes EMT in breast cancer cells as well as metastatic tumor formation via mesenchymal-epithelial transition (MET) in sarcomas (33). Given these functions, and considering the apparent change in morphology seen when growing cells in low serum, we asked whether ΔYB-1 cells have altered expression of EMT/MET-associated factors. WT and ΔYB-1 cells were grown in 10% or 0.1% serum for 3 days and then immunoblotted for Twist1, Zeb1, Snail1, the key transcription factors regulating both EMT and MET (34,35), or for G3BP1, a key regulator of SG formation. Under normal growth conditions (10% serum), cells lacking YB-1 express reduced levels of Twist1 and Snail1 relative to WT controls (Figure 3C, c.f. lane 1 and 3). Under starvation conditions (0.1% serum), cells lacking YB-1 express more Twist1 than do WT controls (Figure 3C, c.f. lane 2 and 4), a finding that may contribute to altered cell morphology. In contrast, expression of Snail1 or G3BP1 is not altered by YB-1 or serum conditions. Consistent with elevated Twist1-induced expression, ΔYB-1 cells grow extremely slowly under low serum conditions (Figure 3D).

Stress granule formation in ΔYB-1 cells

We next compared the SG response in WT and ΔYB-1 cells treated with oxidative (sodium arsenite, 100 μM) or endoplasmic reticulum (thapsagargin, 1 μM) stress by monitoring SG formation using multiple SG markers (eIF4G, G3BP1 and TIAR) with immunofluorescence microscopy. Overall, YB-1 is not required for SG formation triggered by either sodium arsenite or thapsigargin (Figure 4). In dose response experiments, YB-1 deletion slightly impaired SG formation at low concentrations (75 μM) of sodium arsenite (a representative quantification is shown in Figure 4B; we were not able to quantify this data across experiments as the concentration at which 100% of cells formed SA-induced SGs were slightly different in each condition). In response to all tested concentrations of thapsigargin, ΔYB-1 cells were only able to form stress granules in ∼40% of cells indicating some defect in ER stress-mediated SG assembly (Figure 4C). These data demonstrates that YB-1 can promote SG assembly in response to some types of stress, an effect unrelated to reduced expression of G3BP1.

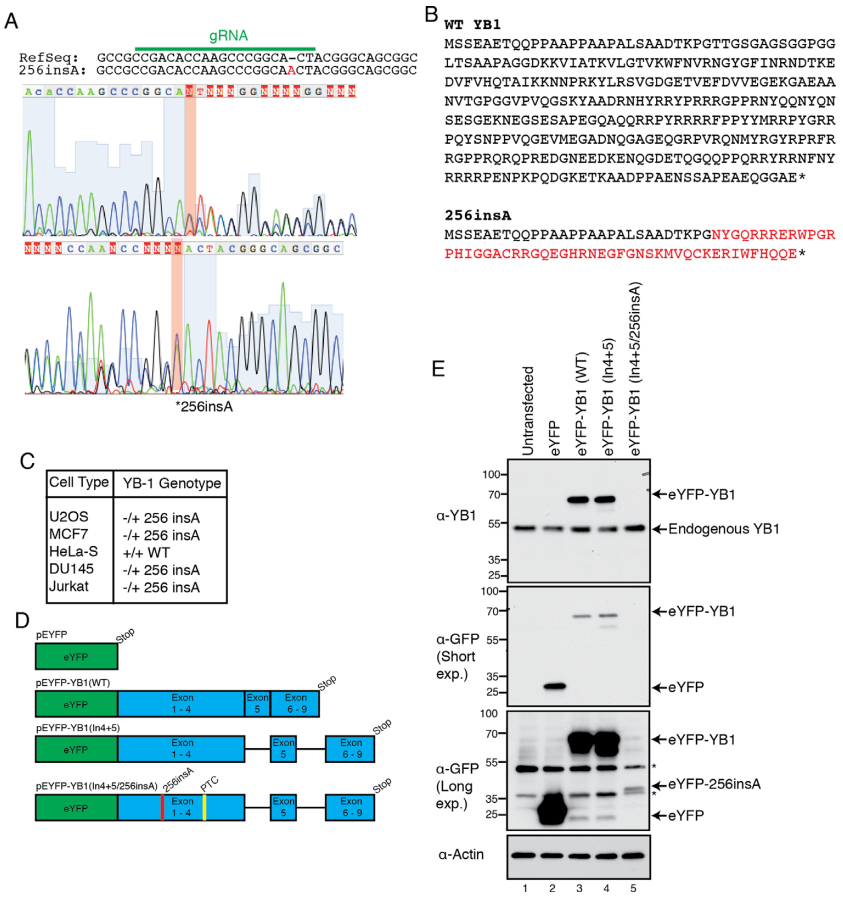

Figure 2. Naturally occurring YB-1 mutations (**A**) Sequencing of YB-1 genomic locus reveals that U2OS cells are heterozygous for a single nucleotide insertion (256insA) within the first exon. Point of insertion is highlighted in red. (**B**) 256insA leads to a frame shift mutation that results in a truncated protein whose mRNA is likely degraded via the nonsense mediated decay pathway. Amino acids downstream of insertion, which diverge from YB-1 sequence, are highlighted in red. (**C**) U2OS, DU145 and MCF7 cells are all heterozygous for 256insA mutation, while HeLa-S cells are homozygous wild-type. (**D**) Schematized YFP-YB1 reporters used to determine if 256insA protein accumulates in cells. (**E**) Western blotting of U2OS transfected with YFP-YB1 reporters demonstrates that 256insA upstream of 2 endogenous introns severely attenuates accumulation of this protein 2 days post transfection.

YB-1 is required for 5′-tiRNA^{Ala}-mediated stress granule formation

5′-TOG-containing 5′-tiRNAs (5′-tiRNA^{Ala} and 5′-tiRNA^{Cys}) promote the assembly of SGs in a phospho-eIF2α independent manner (7). Previous work in our lab suggested that YB-1 is a mediator of SG formation in response to 5′-tiRNA^{Ala} (9), correlating with YB-1-dependent translational repression. Using our ΔYB-1 cells, we asked to what extent YB-1 is required for 5′-tiRNA^{Ala}-mediated SG formation. We found that transfection of 5′-tiRNA^{Ala} induces SG assembly in WT but not ΔYB-1 cells (Figure 5A), consistent with a role for YB-1 in tiRNA-mediated translation repression and SG formation. UV-crosslinking experiments indicate that YB-1 directly binds to 4-thiouridine (4^{S}U)-labeled 5′-tiRNA^{Ala} (12). The YB-1 CSD is likely responsible for specific binding to 5′-TOG-bearing tiRNAs, although non-specific binding through its oligomerization domain may also contribute to this interaction. CSDs are evolutionary conserved nucleic acid binding domains (13). The CSD of YB-1 is highly similar to that of Lin28A and Lin28B (Figure 5B). In particular, a phenylalanine residue in Lin28A that is required for binding to Let-7 pre-miRNAs is conserved in YB-1. Modelling of the YB-1 CSD using solved crystal structures of Lin28A suggested that a binding pocket formed by YB-1 Phe85 could coordinate nucleotides within the 5′-tiRNA^{Ala} D-loop (Figure 5C). Therefore, we expressed and purified recombinant truncated YB-1 (amino acids 1-129) with WT CSD or harbouring a Phe to Ala mutation (F85A), both lacking the oligomerization domain (Supplementary Figure S1A). EMSAs demonstrate that the Phe85 residue is absolutely required for specific RNA binding to 5′-tiRNA^{Ala} (Figure 5D).

To determine whether F85 contributes to YB-1 binding to tiRNAs in cells, we reconstituted the ΔYB-1 U2OS cells with YFP-YB1 (WT), YFP-YB1 (F85A) or free YFP (Figure 5E), and obtained clonally selected reconstituted cell lines. YFP-YB1 (WT) localized to SGs upon oxidative stress (Figure 5F) and to P-bodies under basal conditions (Figure 5G) in accordance with previously reported activities of endogenous YB-1 (36). Remarkably, the F85A mutation dramatically re-localized YFP-YB1 to the nucleus (Figure 5H and I), and YFP-YB1(F85A) only weakly associated with SGs in response to oxidative stress (Figure 5H). The major fraction of YFP-YB1(F85A) was nuclear

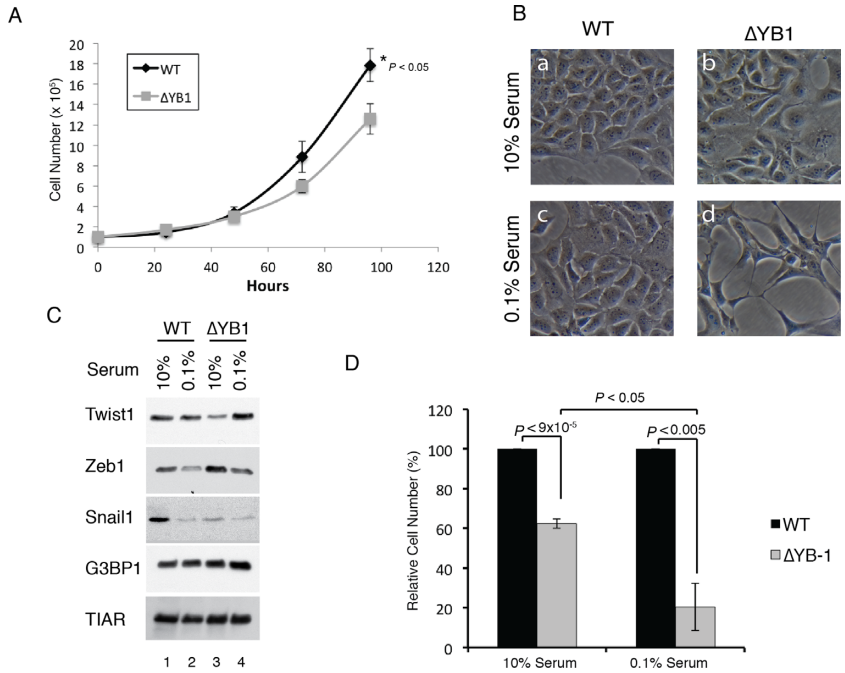

Figure 3. Deletion of YB-1 affects cell growth and survival. (**A**) ΔYB1 U2OS cells grow at an impaired rate as compared to parental U2OS cells. Cell growth was monitored by cell counting over 4 days. Data represent three independent experiments. Error bars are ± standard error. (**B**) Serum starvation of ΔYB1 U2OS cells causes dramatic morphological changes not seen in parental U2OS cells. Cells grown in 10% (Ba and Bb) or 0.1% (Bc and Bd) serum for 3 days are shown (phase-contrast images). (**C**) Levels of EMT/MET-associated factors (Snail1, Twist1) are changed under optimal conditions and in response to serum starvation in ΔYB1 U2OS cells. G3BP1 levels remain unaltered in response to serum starvation. TIAR serves as a loading control. (**D**) ΔYB1 U2OS cells growth/survival is impaired in response to serum starvation. Indicated cells were grown in 10% or 0.1% serum for 7 days and manually counted. Data represent three independent experiments. Error bars are ± standard error.

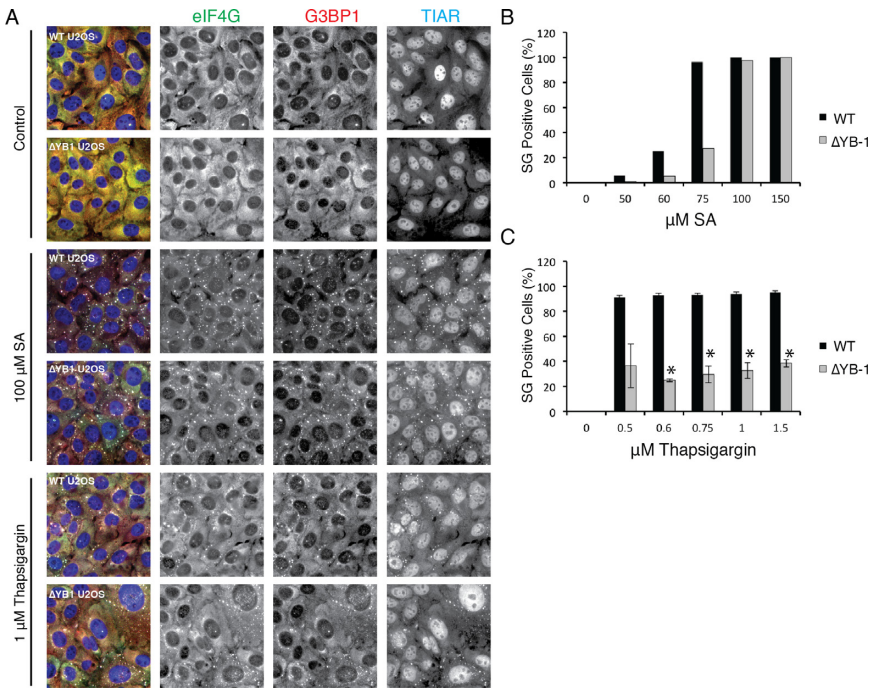

Figure 4. YB-1 depletion does not inhibit sodium arsenite-induced SG formation. (**A**) ΔYB1 U2OS cells are competent to form SGs in response to 100 μM sodium arsenite or 1 μM Thapsigargin (1 h). SG formation was monitored by immunofluorescence of classic SG markers, eIF4G, G3BP1 and TIAR. (**B**) A representative example of quantification of SG formation following a titration of sodium arsenite for 1 h revealing a slight delay in SG assembly in ΔYB1 U2OS cells. Immunofluorescence was used to visualize SG markers (eIF4G, G3BP1 and TIAR). Cells were scored as SG positive if they contained at least 3 foci co-localizing all three markers. (**C**) Quantification of SG formation in response to a titration of thapsigargin (1 h) shows an impaired ability to form SGs in a subset of cells. Cells were imaged by indirect immunofluorescence was used to visualize SG markers (eIF4G, G3BP1 and TIAR). Cells were scored as SG-positive if they contained at least 3 foci co-localizing all three markers (* *P*-value <0.05, n=3).

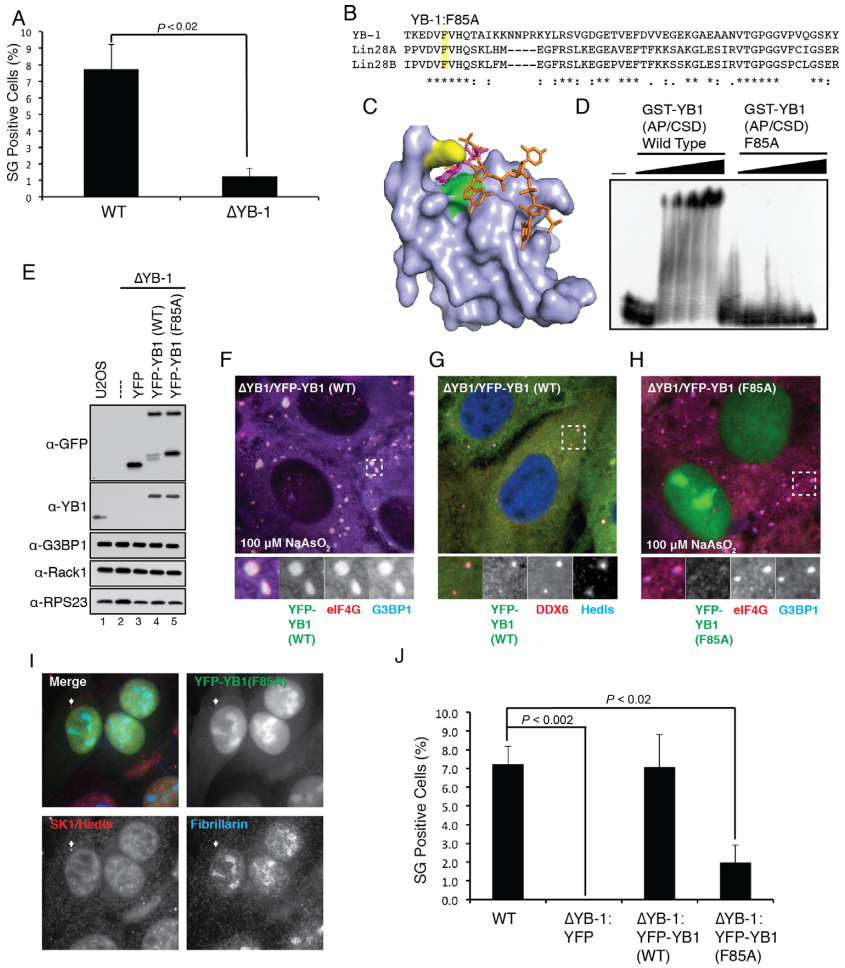

Figure 5. YB-1 is required for 5′-tiRNA^{Ala}-induces stress granule formation. (**A**) Quantification of SG formation in response to 5′-tiRNA^{Ala} demonstrates a blockage in SG formation. Cells were transfected with 100 pmol of 5′-tiRNA^{Ala} for 6 h and SG were visualized by indirect immunofluorescence with SG markers (eIF4G, G3BP1 and TIAR). (**B**) Conservation of cold shock domain (CSD) of YB-1, Lin28A and Lin28B demonstrates conservation of the key phenylalanine residue required for Lin28:let-7 microRNA interaction (49). (**C**) Modeling of YB-1 CSD based on the Lin28 crystal structure reveals a binding pocket utilizing Phe85 (yellow) that could bind 5′-tiRNA^{Ala} (orange). (**D**) Mutation of Phe85 to Alanine (F85A) prevents binding of YB-1 to 5′-tiRNA^{Ala} in an EMSA. Recombinant YB-1 (1–129) was expressed and purified from *E. coli.* Titration (0–500 pmol) of the recombinant YB-1 protein was used to shift 0.25 pmol of [^{32}P]-radiolabeled 5′-tiRNA^{Ala}. (**E**) Generation of ΔYB-1 U2OS cells reconstituted with YFP, YFP-YB1 (WT) or YFP-YB1 (F85A). Expression of YFP tagged constructs were analyzed by GFP and YB-1 antibodies. * indicated breakdown products from YFP tagged YB-1 constructs detected in GFP Western blotting. Reconstitution did not alter G3BP1 expression. Rack1 and RPS23 serve as loading controls. (**F**) YFP-YB1 (WT) localizes to SG following oxidative stress induced by 100 μM sodium arsenite treatment for 1 h as indicated by co-localization with eIF4G and G3BP1. (**G**) YFP-YB1 (WT) localizes to P-bodies under basal conditions as indicated by colocalization with DDX6 (rck/p54). (**H**) YFP-YB1 (F85A) weakly localizes to stress granules in response to oxidative stress induced by sodium arsenite (100 μM for 1 h). (**I**) YFP-YB1(F85A) predominantly localizes to the nucleus. Co-staining with Fibrillarin demonstrates high concentrations of YFP-YB1(F85A) within the nucleolus. Co-staining with Hedls demonstrates that YFP-YB1(F85A) fails to localise to P-bodies (arrowhead). (**J**) Reconstitution of ΔYB1 U2OS cells with YFP-YB1(WT) rescues SG formation in response to 5′-tiRNA^{Ala}, while reconstitution with YFP or YFP-YB1(F85A) fails to rescue. Stress granule formation was induced as in Figure 5A.

with particularly high concentrations in the nucleolus as determined by co-staining with Fibrillarin (Figure 5I). YFP-YB1(F85A) also failed to localized to P-bodies under basal conditions as monitored by co-staining with Hedls (Figure 5I). YFP-YB1 (WT) fully restored tiRNA^{Ala}'s ability to trigger SG formation; whereas reconstitution with free YFP or YFP-YB1(F85A) failed to rescue SGs (Figure 5J). Therefore, YB-1 is required for 5′-tiRNA^{Ala}-induced SG formation and its binding to 5′-tiRNA^{Ala} is required for this function.

YB-1 is not required for 5′-tiRNA^{Ala}-mediated translation repression

We next sought to determine if YB-1 is required for inhibition of translation. We previously showed that 5′-tiRNA^{Ala} inhibits translation initiation by displacing eIF4F from the 5′ mRNA cap (9). To determine if YB-1 is required for displacement of eIF4F from m^{7}GTP, we purified eIF4F and associated proteins, including YB-1, on m^{7}GTP-agarose. Pre-formed complexes were then challenged with control RNA, inactive 5′-tiRNA^{Met} or active 5′-tiRNA^{Ala}. Despite an inability to form SGs in response to 5′-tiRNA^{Ala}, eIF4F

complexes from ΔYB-1 cells are displaced from m^7GTP cap as efficiently as eIF4F complexes from WT cells (Figure 6A). To extend this analysis, we prepared *in vitro* translation lysates from WT or ΔYB-1 cells and analyzed the ability of 5′-tiRNA^{Ala} to inhibit the translation of an mRNA luciferase reporter in these systems (37). Translation of the reporter mRNA was equally repressed in both lysates (Figure 6B), providing further evidence that YB-1 is not required for inhibition of translation in response to 5′-tiRNA^{Ala}, despite being required for SG formation (Figure 5A). We have previously shown that transfection of 5′-tiRNA^{Ala} modestly inhibits translation in U2OS cells. To determine if YB-1 contributes to this effect, we transfected 5′-tiRNA^{Ala} into WT or ΔYB1 U2OS cells and quantified incorporation of puromycin into the proteome following a 5-min pulse. In agreement with *in vitro* data, ablation of YB-1 in U2OS cells did not significantly affect 5′-tiRNA^{Ala}-mediated translational repression (Figure 6C and D). In cells, it is possible that YB-1 protects tiRNAs from exonucleolytic degradation; however, as loss of YB-1 does not alter the functionality of 5′-tiRNA^{Ala}, it is unlikely that it alters its stability. Further, G-quadruplex-like structures, like those found at the 5′ end of 5′-tiRNA^{Ala}, are intrinsically insensitive to nucleolytic attack, as are 2′–3′ cyclic phosphates found at the 3′ end of 5′-tiRNA^{Ala}.

DISCUSSION

tRNA cleavage is an evolutionarily conserved phenomenon serving various functions in different organisms (38–40). In mammalian cells, tRNA cleavage is involved in a cellular stress response program that enhances cell survival under stress. We showed the ribonuclease ANG is activated to produce tiRNAs that act at the post-transcriptional level to re-program cellular translation (8). Selected 5′-tiRNAs (5′-tiRNA^{Ala} and 5′-tiRNA^{Cys}) containing 5′-TOG motifs and assembling G-quadruplex-like structures are potent inhibitors of translation (12). On the molecular level, these 5′-TOG-tiRNAs interfere with assembly of the cap-binding eIF4F complex to inhibit translation initiation (9). On the cellular level, and as a consequence of translation repression, tiRNAs promote the assembly of cytoprotective SGs (7). Biochemical approaches identified the known translational silencer YB-1 as a direct partner of 5′-TOG tiRNAs. Here we demonstrate that YB-1 is required for the tiRNA-induced assembly of SGs, but not for tiRNA-mediated translation inhibition.

YB-1 has long been recognized as a potential oncogene (18,32). YB-1 is overexpressed in multiple cancer types and its increased expression is associated with increased invasiveness (17). This function has been partially attributed to YB-1's ability to promote the translation of EMT/MET-associated factors, such as Snail1 and Twist1 (20,21), while simultaneously inhibiting the translation of other cellular mRNAs (41). Such YB-1-mediated reprogramming of cellular translation contributes to cancer cell survival and transformation. In the Evdokimova *et al*. study (21), overexpression of ectopic YB-1 led to increased Snail1 and Twist1 expression with consequent transformation of non-invasive breast cancer cells into malignant carcinomas. Here, in the reciprocal experiment, we demonstrate that CRISPR/Cas9-based ablation of YB-1 leads to reduced expression of Snail1 and Twist1 proteins (Figure 3C, c.f. lanes 1 and 3), supporting YB-1's proposed role in EMT. Further, this correlates with diminished proliferative capacity of ΔYB-1 U2OS cells (Figure 3A) and decreased survival in response to serum-starvation (Figure 3D). These data further highlight the pro-proliferative effects of YB-1 that support tumor growth and survival.

While the role of YB-1 in EMT and epithelial malignancies is well established, recent reports also suggest that YB-1 drives metastasis in sarcomas, malignancies of mesenchymal origin. This role may be attributed to YB-1 functions in the regulation of Snail1/Twist/ZEB1 transcription factors, the factors that are implicated in both EMT of epithelial cancers and MET of sarcomas (34). Moreover, two recent reports from the Sorensen lab (22,33) demonstrated that YB-1 overexpression positively correlates with carcinoma progression and metastatic dissemination as well as its elevation in high-risk sarcomas and association with poor outcome. Both reports suggest that YB-1 promotes tumor progression by translational activation of its mRNA targets, namely *HIF1α* and/or *G3BP1* transcripts. As a result of YB-1 dependent HIF1α up-regulation cancer cells adapt to hypoxia, a stress condition that plays a dominant role in tumor invasion and metastasis. Similarly, translational activation of G3BP1 expression also promotes adaptation to cellular stresses. Samasekharan *et al*. reported that YB-1 promotes tumor progression via G3BP1-mediated SG formation (22). While the role of G3BP1 in the promotion of SGs is well documented (42,43), our data suggest that YB-1 regulates SG formation in a more complex and stress-specific manner. In contrast to Samasekharan *et al*. (22), our results do not support a direct role for YB-1 in the regulation of G3BP1 expression since siRNA- and CRISPR/Cas9-mediated YB-1 depletion does not affect expression of G3BP1. This difference may be attributed to the known heterogeneity of U2OS cells that results from defects in the maintenance of cell ploidy (44). We do observe that YB-1 depletion modestly delays sodium arsenite-induced SG assembly (Figure 4B) as reported in their study. Interestingly, YB-1 depletion strongly affects thapsigargin- and dominantly down-regulates tiRNA- mediated SG formation (Figures 4C and 5).

The prevalence of a single nucleotide insertion in the first exon of YB-1 is striking. Four of the five cell lines tested were found to possess this heterozygous mutation. This frameshift mutation (256insA) creates a PTC in the second exon. Translation of this mRNA would lead to an 8-kDa protein sharing only the first 27 amino acids with YB-1. Our data suggest that this protein does not accumulate to the same extent as endogenous YB-1. The mRNA is likely degraded by the nonsense mediated mRNA decay pathway (45) (due to the presence of six exon junctions downstream of the PTC), resulting in mRNA degradation and minimal production of this truncated protein. NMD functions to clear the cell of mRNAs that could code for toxic non-functional C-terminally truncated proteins. However, there are several instances of 'NMD escape' in which NMD targets are not efficiently cleared thereby allowing for the synthesis of toxic protein products. Our data show that the 256insA mutation severely reduces the levels of a reporter

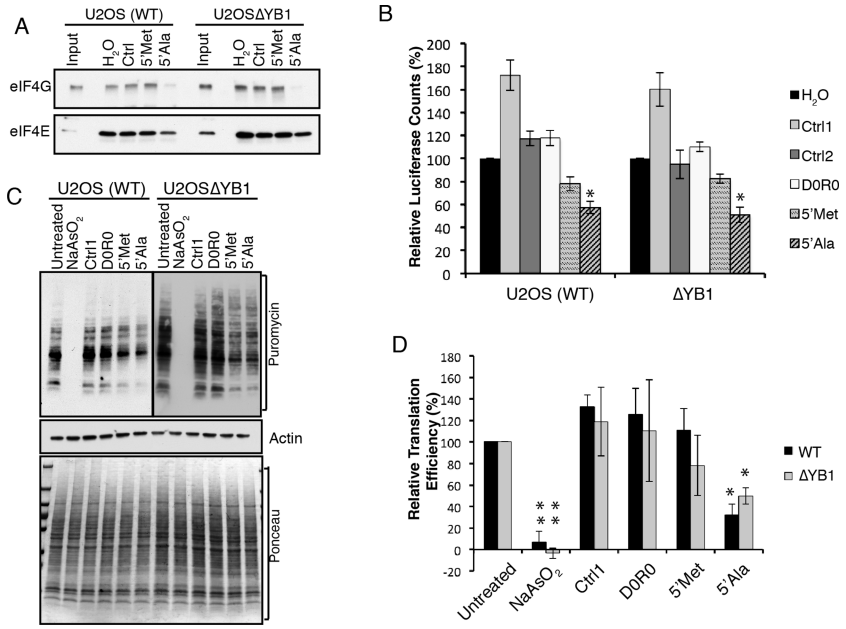

Figure 6. YB-1 is dispensable for 5′-tiRNA^{Ala}-induced eIF4F disassembly and translation inhibition (**A**) Genetic ablation of YB-1 does not affect ability of 5′-tiRNA^{Ala} to displace eIF4F from m^{7}GTP. A total of 100 pmol of the indicated RNA was added to eIF4F preformed onto m^{7}GTP-agarose. 5′-tiRNA^{Ala} was able to displace eIF4G and a portion of eIF4E in both WT or ΔYB-1 Lysates (c.f. lane 5 and 10). (**B**) *In vitro* translation assays utilizing cell lysates from WT U2OS or ΔYB-1 U2OS. Efficiency of uncapped *Renilla* luciferase mRNA translation was monitored by luminescence. Addition of 5′-tiRNA^{Ala} to *in vitro* translation lysate inhibited the translation of the luciferase mRNA to the similar extents in both WT and ΔYB-1 U2OS lysates (*- p-value =0.0004, n=4). (**C**) 5′-tiRNA^{Ala} represses global translation in both WT and ΔYB1 U2OS cells. Cells were transfected with 100 pmol of indicated RNAs for 6 h. Cells were pulsed with puromycin to a final concentration of 5 μg/ml for 5 min. Cells were lysed in 1% SDS, 5 mM MES [pH 6.5] to ensure translation does not continue during lysis. Relative translation efficiency was analyzed by western blotting for puromycin incorporated into the proteome. Ponceau staining and actin levels serve as a loading control. Treatment of cells with 100 μM sodium arsenite for 1 h previous to puromycin labelling serves as a control for inhibition of translation and specificity of puromycin antibody. (**D**) Quantification of relative incorporation of puromycin into protein (n = 3) normalized to actin. * is $P < 0.003$. ** is $P < 0.0007$.

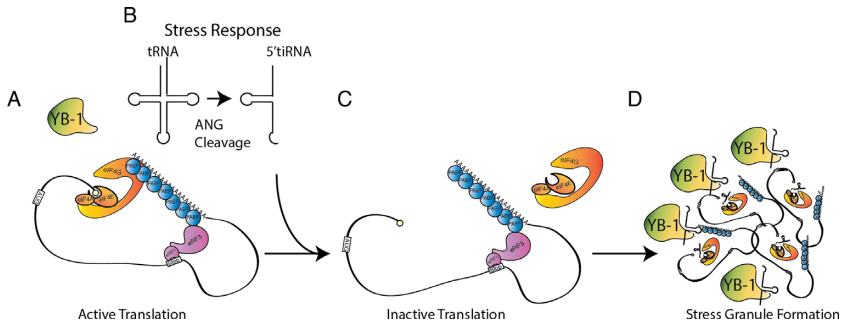

Figure 7. Model of YB-1's involvement in tiRNA-mediated stress response pathway. (**A**) Actively translating mRNA is circularized through the interaction of eIF4F (orange), PABP (blue), translation termination factors eRF1/eRF3 (pink). (**B**) During stress, tRNAs are cleaved by ANG creating 5′-tiRNAs which displace eIF4F from m^{7}GTP cap of mRNA (**C**), thereby inhibiting translation initiation. (**D**) YB-1 (green-orange) acts to package inactive mRNPs, inhibited through the action of 5′-tiRNAs, into SGs.

harbouring the mutation (Figure 2). However, some protein product remains and therefore, it is possible that it may have some unidentified cellular effect.

It is unclear how the loss of one YB-1 allele will affect cellular function. YB-1 autoregulates its own expression by binding to the 5′UTR of *YB-1* mRNA and inhibiting translation (46). Therefore, a 50% reduction of *YB-1* mRNA may affect levels of YB-1 protein through inhibition of its own mRNA translation. The prevalence of the 256insA mutation in commonly grown cancer lines implies that this alteration confers a growth or survival advantage. Given the documented roles of YB-1 and ANG in carcinogenesis, it is tempting to speculate that this mutation reduces the expression of YB-1 and/or YB-1:tiRNA complexes. Such dysregulation may affect the ability of tiRNAs and or YB-1 to re-program cellular translation/formation of SGs and predispose cells toward a cancerous state.

ANG, the ribonuclease responsible for 5′-tiRNA biogenesis, is also upregulated in many cancers. The effects of YB-1 on mRNA translation overlap significantly with effects of tiRNAs on translation. Both YB-1 and 5′-TOG-tiRNAs are repressors of cap-dependent translation (18). It has been suggested that YB-1 modulates translation initiation by preventing association of eIF4G with the m^{7}GTP

mRNA cap (16,47) and/or by stabilization of eIF4F on the m^7GTP cap (15). Similarly, 5′-TOG-containing tiRNAs displace eIF4G/E from the m^7GTP cap. We previously reported that YB-1 interacts with 5′-TOG-containing tiRNAs in cell lysates (12). Our EMSA analysis using purified YB-1 and synthetic tiRNAs confirmed these direct interactions (Figure 5B–D). Moreover, we show that a conserved Phe85 residue in the CSD of YB-1 is responsible for the interaction and a Phe-85-Ala mutation completely abolishes binding of YB-1 to tiRNAs (Figure 5, and not shown). As tiRNAs interact with YB-1, and siRNA-based depletion of YB-1 decreases the ability of tiRNAs to promote SGs, we initially hypothesized that YB-1:tiRNA complexes may directly inhibit translation initiation. This hypothesis has been refuted by three observations: (i) genetic ablation of YB-1 in U2OS cells does not alter the ability of 5′-tiRNAs to displace eIF4F components from the m^7GTP cap, (ii) an *in vitro* translation system using cell lysates prepared from WT and ΔYB-1 U2OS cells reveals that 5′-tiRNA^{Ala} inhibits mRNA translation of a luciferase reporter in a YB-1 independent manner, and (iii) global translation is reduced in response to 5′-tiRNA^{Ala} in ΔYB-1 U2OS cells.

YB-1 is required for SG formation in response to tiRNAs. Following inhibition of translation initiation, stalled 48S pre-initiation complexes condense into SGs (48). This occurs through a two-step process. Following translation inhibition, polysomes disassemble leading to a sudden influx of untranslated mRNPs. At this stage, protein synthesis has ceased, but discrete SGs have not yet assembled. The 2nd step of SG formation involves the actions of aggregation-prone proteins possessing low complexity motifs (e.g. G3BP1/2, TIA1/R, etc.) that support a liquid phase translation required for SG assembly. As this step of SG formation is impaired by the loss of YB-1 in response to 5′-tiRNA^{Ala} (Figure 5), we propose that YB-1 works as an 'RNA chaperone' to help packaging mRNA inhibited by tiRNAs into SGs. Components of eIF4F are still displaced from m^7GTP and translation is inhibited in the absence of YB-1, but naked mRNA is unable to be packed into SGs. An appealing scenario is that tiRNA binding to the YB-1 CSD promotes a conformational change that allows for increased non-specific RNA binding affinity or multimerization through the OMD. In agreement with this hypothesis, reconstitution of ΔYB1 U2OS cells with wild-type YB-1, but not with F85A YB-1, rescues 5′-tiRNA^{Ala} mediated SG formation. Because 5′-tiRNA^{Ala} triggers SG formation through an eIF2α phosphorylation independent mechanism, other SG nucleating proteins (e.g. G3BP1) are not activated and therefore cannot compensate for loss of YB-1.

We propose the following model for 5'-tiRNA^{Ala} function during the stress response. Under normal growth conditions, polysomes form a closed-loop translation complex mediated by interaction with eIF4G and PABP (Figure 7A). In response to stress, tRNAs are cleaved within the anticodon loop by ANG, creating 5′- and 3′-tiRNAs, of which a subset of 5′-TOG-containing tiRNAs have bioactivity (Figure 7B). 5′TOG-containing tiRNAs facilitate the displacement of eIF4F from the mRNA cap, disrupting translation initiation (Figure 7C). Stalled translation complexes condense into SGs mediated by 5′-tiRNA^{Ala} bound to the CSD of YB-1 (Figure 7D). An unresolved question is the mechanism by which tiRNA^{Ala} promotes eIF4F disassembly to repress translation. If the YB-1:tiRNA mRNP complex does not directly act on eIF4F, does 5′tiRNA^{Ala} assemble into other complexes that promote this activity? Alternatively, are there additional components of the YB-1:tiRNA complex yet to be discovered? Future investigations will elucidate the answer to this question.

SUPPLEMENTARY DATA

Supplementary Data are available at NAR Online.

ACKNOWLEDGEMENT

The authors thank members of Ivanov and Anderson labs for technical support and helpful comments. We thank Dr Ilya M. Terenin and Dr Sergey E. Dmitriev (Belozersky Institute of Physico-Chemichal Biology, Lomonosov Moscow State University, Moscow, Russia) for their help in establishing *in vitro* mRNA translation assay from cultured cells.

FUNDING

National Institutes of Health [GM111700 and CA168872 to P.A., NS094918 to P.I., GM119283 to S.L.]. Funding for open access charge: National Institutes of Health (NIH), USA (NS094918).
Conflict of interest statement. None declared.

REFERENCES

1. Yamasaki,S. and Anderson,P. (2008) Reprogramming mRNA translation during stress. *Curr. Opin. Cell Biol.*, **20**, 222–226.
2. Holcik,M. and Sonenberg,N. (2005) Translational control in stress and apoptosis. *Nat. Rev. Mol. Cell Biol.*, **6**, 318–327.
3. Kedersha,N., Ivanov,P. and Anderson,P. (2013) Stress granules and cell signaling: more than just a passing phase? *Trends Biochem. Sci.*, **38**, 494–506.
4. Anderson,P., Kedersha,N. and Ivanov,P. (2015) Stress granules, P-bodies and cancer. *Biochim. Biophys. Acta*, **1849**, 861–870.
5. Bordeleau,M.E., Matthews,J., Wojnar,J.M., Lindqvist,L., Novac,O., Jankowsky,E., Sonenberg,N., Northcote,P., Teesdale-Spittle,P. and Pelletier,J. (2005) Stimulation of mammalian translation initiation factor eIF4A activity by a small molecule inhibitor of eukaryotic translation. *Proc. Natl. Acad. Sci. U.S.A.*, **102**, 10460–10465.
6. Bevilacqua,E., Wang,X., Majumder,M., Gaccioli,F., Yuan,C.L., Wang,C., Zhu,X., Jordan,L.E., Scheuner,D., Kaufman,R.J. *et al.* (2010) eIF2alpha phosphorylation tips the balance to apoptosis during osmotic stress. *J. Biol. Chem.*, **285**, 17098–17111.
7. Emara,M., Ivanov,P., Hickman,T., Dawra,N., Tisdale,S., Kedersha,N., Hu,G. and Anderson,P. (2010) Angiogenin-induced tiRNAs promote stress-induced stress granule assembly. *J. Biol. Chem.*, **285**, 10959–10968.
8. Yamasaki,S., Ivanov,P., Hu,G.F. and Anderson,P. (2009) Angiogenin cleaves tRNA and promotes stress-induced translational repression. *J. Cell Biol.*, **185**, 35–42.
9. Ivanov,P., Emara,M.M., Villen,J., Gygi,S.P. and Anderson,P. (2011) Angiogenin-Induced tRNA Fragments Inhibit Translation Initiation. *Mol. Cell*, **43**, 613–623.
10. Fu,H., Feng,J., Liu,Q., Sun,F., Tie,Y., Zhu,J., Xing,R., Sun,Z. and Zheng,X. (2009) Stress induces tRNA cleavage by angiogenin in mammalian cells. *FEBS Lett.*, **583**, 437–442.
11. Saikia,M., Krokowski,D., Guan,B.J., Ivanov,P., Parisien,M., Hu,G.F., Anderson,P., Pan,T. and Hatzoglou,M. (2012) Genome-wide identification and quantitative analysis of cleaved tRNA fragments induced by cellular stress. *J. Biol. Chem.*, **287**, 42708–42725.

12. Ivanov,P., O'Day,E., Emara,M.M., Wagner,G., Lieberman,J. and Anderson,P. (2014) G-quadruplex structures contribute to the neuroprotective effects of angiogenin-induced tRNA fragments. *Proc. Natl. Acad. Sci. U.S.A.*,**111**, 18201–18206.
13. Mihailovich,M., Militti,C., Gabaldon,T. and Gebauer,F. (2010) Eukaryotic cold shock domain proteins: highly versatile regulators of gene expression. *BioEssays*, **32**, 109–118.
14. Skabkin,M.A., Kiselyova,O.I., Chernov,K.G., Sorokin,A.V., Dubrovin,E.V., Yaminsky,I.V., Vasiliev,V.D. and Ovchinnikov,L.P. (2004) Structural organization of mRNA complexes with major core mRNP protein YB-1. *Nucleic Acids Res.*, **32**, 5621–5635.
15. Evdokimova,V., Ruzanov,P., Imataka,H., Raught,B., Svitkin,Y., Ovchinnikov,L.P. and Sonenberg,N. (2001) The major mRNA-associated protein YB-1 is a potent 5′ cap-dependent mRNA stabilizer. *EMBO J.*, **20**, 5491–5502.
16. Nekrasov,M.P., Ivshina,M.P., Chernov,K.G., Kovrigina,E.A., Evdokimova,V.M., Thomas,A.A., Hershey,J.W. and Ovchinnikov,L.P. (2003) The mRNA-binding protein YB-1 (p50) prevents association of the eukaryotic initiation factor eIF4G with mRNA and inhibits protein synthesis at the initiation stage. *J. Biol. Chem.*, **278**, 13936–13943.
17. Chatterjee,M., Rancso,C., Stuhmer,T., Eckstein,N., Andrulis,M., Gerecke,C., Lorentz,H., Royer,H.D. and Bargou,R.C. (2008) The Y-box binding protein YB-1 is associated with progressive disease and mediates survival and drug resistance in multiple myeloma. *Blood*, **111**, 3714–3722.
18. Eliseeva,I.A., Kim,E.R., Guryanov,S.G., Ovchinnikov,L.P. and Lyabin,D.N. (2011) Y-box-binding protein 1 (YB-1) and its functions. *Biochemistry (Mosc)*, **76**, 1402–1433.
19. Kohno,K., Izumi,H., Uchiumi,T., Ashizuka,M. and Kuwano,M. (2003) The pleiotropic functions of the Y-box-binding protein, YB-1. *BioEssays*, **25**, 691–698.
20. Khan,M.I., Adhami,V.M., Lall,R.K., Sechi,M., Joshi,D.C., Haidar,O.M., Syed,D.N., Siddiqui,I.A., Chiu,S.Y. and Mukhtar,H. (2014) YB-1 expression promotes epithelial-to-mesenchymal transition in prostate cancer that is inhibited by a small molecule fisetin. *Oncotarget*, **5**, 2462–2474.
21. Evdokimova,V., Tognon,C., Ng,T., Ruzanov,P., Melnyk,N., Fink,D., Sorokin,A., Ovchinnikov,L.P., Davicioni,E., Triche,T.J. *et al.* (2009) Translational activation of snail1 and other developmentally regulated transcription factors by YB-1 promotes an epithelial-mesenchymal transition. *Cancer Cell*, **15**, 402–415.
22. Somasekharan,S.P., El-Naggar,A., Leprivier,G., Cheng,H., Hajee,S., Grunewald,T.G., Zhang,F., Ng,T., Delattre,O., Evdokimova,V. *et al.* (2015) YB-1 regulates stress granule formation and tumor progression by translationally activating G3BP1. *J. Cell Biol.*, **208**, 913–929.
23. Kedersha,N. and Anderson,P. (2007) Mammalian stress granules and processing bodies. *Methods Enzymol.*, **431**, 61–81.
24. Nelson,M.D. and Fitch,D.H. (2011) Overlap extension PCR: an efficient method for transgene construction. *Methods Mol. Biol.*, **772**, 459–470.
25. Lyons,S.M., Ricciardi,A.S., Guo,A.Y., Kambach,C. and Marzluff,W.F. (2014) The C-terminal extension of Lsm4 interacts directly with the 3′ end of the histone mRNP and is required for efficient histone mRNA degradation. *RNA*, **20**, 88–102.
26. Andreev,D.E., Dmitriev,S.E., Terenin,I.M., Prassolov,V.S., Merrick,W.C. and Shatsky,I.N. (2009) Differential contribution of the m7G-cap to the 5′ end-dependent translation initiation of mammalian mRNAs. *Nucleic Acids Res.*, **37**, 6135–6147.
27. Ran,F.A., Hsu,P.D., Wright,J., Agarwala,V., Scott,D.A. and Zhang,F. (2013) Genome engineering using the CRISPR-Cas9 system. *Nat. Protoc.*, **8**, 2281–2308.
28. Mali,P., Yang,L., Esvelt,K.M., Aach,J., Guell,M., DiCarlo,J.E., Norville,J.E. and Church,G.M. (2013) RNA-guided human genome engineering via Cas9. *Science*, **339**, 823–826.
29. Wu,K., Chen,K., Wang,C., Jiao,X., Wang,L., Zhou,J., Wang,J., Li,Z., Addya,S., Sorensen,P.H. *et al.* (2014) Cell fate factor DACH1 represses YB-1-mediated oncogenic transcription and translation. *Cancer Res.*, **74**, 829–839.
30. Kedersha,N., Panas,M.D., Achorn,C.A., Lyons,S., Tisdale,S., Hickman,T., Thomas,M., Lieberman,J., McInerney,G.M., Ivanov,P. *et al.* (2016) G3BP-Caprin1-USP10 complexes mediate stress granule condensation and associate with 40S subunits. *J. Cell Biol.*, **212**, 845–860.
31. Hsu,P.D., Scott,D.A., Weinstein,J.A., Ran,F.A., Konermann,S., Agarwala,V., Li,Y., Fine,E.J., Wu,X., Shalem,O. *et al.* (2013) DNA targeting specificity of RNA-guided Cas9 nucleases. *Nat. Biotechnol.*, **31**, 827–832.
32. Lyabin,D.N., Eliseeva,I.A. and Ovchinnikov,L.P. (2014) YB-1 protein: functions and regulation. *Wiley Interdiscip. Rev. RNA*, **5**, 95–110.
33. El-Naggar,A.M., Veinotte,C.J., Cheng,H., Grunewald,T.G., Negri,G.L., Somasekharan,S.P., Corkery,D.P., Tirode,F., Mathers,J., Khan,D. *et al.* (2015) Translational Activation of HIF1alpha by YB-1 Promotes Sarcoma Metastasis. *Cancer Cell*, **27**, 682–697.
34. Yang,J., Du,X., Wang,G., Sun,Y., Chen,K., Zhu,X., Lazar,A.J., Hunt,K.K., Pollock,R.E. and Zhang,W. (2014) Mesenchymal to epithelial transition in sarcomas. *Eur. J. Cancer*, **50**, 593–601.
35. McAllister,S.S. and Weinberg,R.A. (2014) The tumour-induced systemic environment as a critical regulator of cancer progression and metastasis. *Nat. Cell Biol.*, **16**, 717–727.
36. Yang,W.H. and Bloch,D.B. (2007) Probing the mRNA processing body using protein macroarrays and 'autoantigenomics'. *RNA*, **13**, 704–712.
37. Terenin,I.M., Andreev,D.E., Dmitriev,S.E. and Shatsky,I.N. (2013) A novel mechanism of eukaryotic translation initiation that is neither m7G-cap-, nor IRES-dependent. *Nucleic Acids Res.*, **41**, 1807–1816.
38. Gebetsberger,J. and Polacek,N. (2013) Slicing tRNAs to boost functional ncRNA diversity. *RNA Biol.*, **10**, 1798–1806.
39. Thompson,D.M. and Parker,R. (2009) Stressing out over tRNA cleavage. *Cell*, **138**, 215–219.
40. Anderson,P. and Ivanov,P. (2014) tRNA fragments in human health and disease. *FEBS Lett.*, **588**, 4297–4304.
41. Evdokimova,V., Tognon,C., Ng,T. and Sorensen,P.H. (2009) Reduced proliferation and enhanced migration: two sides of the same coin? Molecular mechanisms of metastatic progression by YB-1. *Cell Cycle*, **8**, 2901–2906.
42. Aulas,A., Caron,G., Gkogkas,C.G., Mohamed,N.V., Destroismaisons,L., Sonenberg,N., Leclerc,N., Parker,J.A. and Vande Velde,C. (2015) G3BP1 promotes stress-induced RNA granule interactions to preserve polyadenylated mRNA. *J. Cell Biol.*, **209**, 73–84.
43. Aulas,A., Stabile,S. and Vande Velde,C. (2012) Endogenous TDP-43, but not FUS, contributes to stress granule assembly via G3BP. *Mol. Neurodegener.*, **7**, 54–68.
44. Ben-Shoshan,S.O., Simon,A.J., Jacob-Hirsch,J., Shaklai,S., Paz-Yaacov,N., Amariglio,N., Rechavi,G. and Trakhtenbrot,L. (2014) Induction of polyploidy by nuclear fusion mechanism upon decreased expression of the nuclear envelope protein LAP2beta in the human osteosarcoma cell line U2OS. *Mol. Cytogenet.*, **7**, 9–21.
45. Schweingruber,C., Rufener,S.C., Zund,D., Yamashita,A. and Muhlemann,O. (2013) Nonsense-mediated mRNA decay - mechanisms of substrate mRNA recognition and degradation in mammalian cells. *Biochimica et Biophysica Acta*, **1829**, 612–623.
46. Skabkina,O.V., Lyabin,D.N., Skabkin,M.A. and Ovchinnikov,L.P. (2005) YB-1 autoregulates translation of its own mRNA at or prior to the step of 40S ribosomal subunit joining. *Mol. Cell. Biol.*, **25**, 3317–3323.
47. Svitkin,Y.V., Evdokimova,V.M., Brasey,A., Pestova,T.V., Fantus,D., Yanagiya,A., Imataka,H., Skabkin,M.A., Ovchinnikov,L.P., Merrick,W.C. *et al.* (2009) General RNA-binding proteins have a function in poly(A)-binding protein-dependent translation. *EMBO J.*, **28**, 58–68.
48. Anderson,P. and Kedersha,N. (2009) Stress granules. *Curr. Biol.*, **19**, R397–R398.
49. Nam,Y., Chen,C., Gregory,R.I., Chou,J.J. and Sliz,P. (2011) Molecular basis for interaction of let-7 microRNAs with Lin28. *Cell*, **147**, 1080–1091.